ACS MATERIALS Au
AN OPEN ACCESS JOURNAL OF THE AMERICAN CHEMICAL SOCIETY

pubs.acs.org/materialsau Article

Analysis of Ignition Sites for the Explosives 3,3′-Diamino-4,4′-azoxyfurazan (DAAF) and 1,3,5,7-Tetranitro-1,3,5,7-tetrazoctane (HMX) Using Crush Gun Impact Testing

Nicholas Lease, Matthew D. Holmes, Michael A. Englert-Erickson, Lisa M. Kay, Elizabeth G. Francois,* and Virginia W. Manner*

Cite This: *ACS Mater. Au* 2021, 1, 116–129 Read Online

ACCESS | Metrics & More | Article Recommendations

ABSTRACT: The handling safety characteristics of energetic materials must be measured in order to ensure the safe transport and use of explosives. Drop-weight impact sensitivity measurements are one of the first standardized tests performed for energetics. They utilize a small amount of the explosive sample and a standard weight, which is dropped on the material from various heights to determine its sensitivity. While multiple laboratories have used the impact sensitivity test as an initial screening tool for explosive sensitivity for the past 60 years, variability exists due to the use of different instruments, different methods to determine the initiation, and the scatter commonly associated with less-sensitive explosives. For example, standard explosives such as 1,3,5,7-tetranitro-1,3,5,7-tetrazoctane (HMX) initiate reliably and consistently on the drop-weight impact test, whereas insensitive explosives such as 3,3′-diamino-4,4′-azoxyfurazan (DAAF) exhibit variability in sound levels and the expended material. Herein we investigate the impact sensitivity of DAAF and HMX along with a more detailed investigation of ignition sites using a novel "crush gun" apparatus: a pneumatically powered drop-weight tower with advanced diagnostics, including high-speed visual and infrared cameras. Using this crush gun assembly, the ignition sites in HMX and DAAF were analyzed with respect to the effects of particle size and the presence of a source of grit. The formation of ignition sites was observed in both explosives; however, only HMX showed ignition sites that propagated to a deflagration at lower firing speeds. Finally, the presence of grit particles was shown to increase the occurrence of ignition sites in DAAF at lower firing speeds, though propagation to a full reaction was not observed on the time scale of the test. These results enable a better understanding of how ignition and propagation occurs during the impact testing of DAAF.

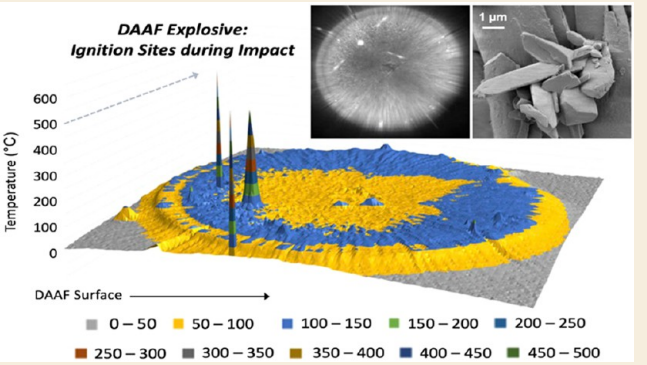

KEYWORDS: *Explosive, DAAF, HMX, Handling Sensitivity, Ignition Site, Crush Gun, Impact, Safety*

INTRODUCTION

The safety and characterization of explosives is necessary for the handling, transport, and design of novel next-generation energetic materials. To ensure the proper handling and storage of each unique energetic material, handling sensitivity tests are conducted in order to assess the material's response to various stimuli, such as thermal, impact, friction, and spark.[1] While computational models and simulations have been developed in order to predict energetic material sensitivity,[2−6] empirical data are still required for accurate assessments. Many methods are available for the sensitivity testing of energetics;[7−9] however, varying analysis and instrumentation can make comparison of those results difficult. Despite efforts by the United Nations to standardize many of these sensitivity tests,[1] variations in testing conditions can result in a range of values for a particular energetic, particularly when it comes to impact testing. Additionally, most of the sensitivity tests that are regularly utilized were designed early in the history of explosives research as simple "go" or "no go" threshold screening criteria and, though useful for safety screening applications, do not directly address the underlying physics of the explosive response that determine violence.

This study focuses on low-velocity impacts (e.g., sub-shock insults), which create localized thermal ignitions, and observes whether they can then potentially transition to a violent

Received: April 29, 2021
Published: July 14, 2021

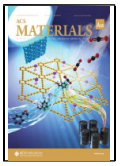

reaction. The United Nations lists six tests to analyze the impact sensitivity of explosives,[10] with the three most common being the BAM Fallhammer test,[11,12] the US drophammer (ERL-type) test,[13,14] and the Rotter test.[15,16] The drop hammer test, the BAM friction test, and ESD testing are conducted with small samples (~40 mg). The impact sensitivity test is typically conducted by lightly confining an explosive sample between an anvil and a steel striker, then dropping a suspended weight on the striker from various heights. The assumption is that a more sensitive material reacts at a lower drop height (lower input of energy). The determination of a "go" is usually accompanied by a flash of light, the generation of gas, sample expenditure, or a sound recorded on audio instrumentation.[17−21] With testing spanning numerous facilities and over 60 years of implementation, large standard deviations exist in collected impact sensitivity data.[22] For example, drop-weight impact measurements of the same energetic materials were shown to have different results when conducted on different instruments.[20,23−25] One reason for the discrepancy is that different facilities implement differing means for determining the reaction of the sample, or a "go".[26,27] It has also been shown that a considerable fraction of the available drop energy is partitioned into the elastic deformation of steel striker and anvil components at the moment that ignition occurs;[28] this necessarily implies that the test outcome is not inherent to the explosive alone but is instead highly dependent on the apparatus configuration.

In addition to variations in experimental setups, the drop-weight apparatus convolves the processes of explosive ignition (the onset of luminous exothermic gas-phase reactions) with post-ignition propagation (deflagration that is sustained through the material) into a single "integrated" test. Despite multiple tests and investigations, the mesoscale processes that allow an ignition to propagate into a violent outcome are still not fully understood. While it has generally been agreed since the 1940's that ignition under drop hammer conditions requires the formation of localized ignition sites,[29−34] followed by visco-plastic shear heating,[35−37] there is lack of consensus concerning the adiabatic heating of gas bubbles entrained in the explosive, the role of melting during the event,[38] the effect of the material particle size,[39,40] and the presence or absence of grit during testing.[41−43] Furthermore, when dealing with less sensitive materials, e.g., 2,4,6-trinitrotoluene (TNT), the determination of a "go" can be more difficult because substantial material remains after the test despite an audible "go".[44] As a result, the test is recommended for ranking explosives within one laboratory and is not generally utilized for the in-depth analysis of the ignition and propagation behavior of explosives.

3,3′-Diamino-4,4′-azoxyfurazan (DAAF) is a furazan-based explosive that has been studied extensively as a potential insensitive high explosive (IHE), a safe explosive that is stable to most common insults. DAAF has recently been investigated for its synthesis,[45−47] physical properties,[48−51] explosive sensitivity,[52] particle morphology,[47] explosive properties,[52,53] and plastic-bonded formulations (PBX).[54] Recently, we reported drop-weight impact test data on different particle sizes of DAAF both with and without the use of grit paper.[6] Surprisingly, audible "go" responses were recorded at drop height values lower than expected for an insensitive energetic. To investigate this further, herein we report the imaging of DAAF during subshock impacts along with the more sensitive standard explosive HMX (1,3,5,7-tetranitro-1,3,5,7-tetrazoctane) (Scheme 1) in order to probe the ignition and propagation behavior that occur during the drop hammer test. Using an improved pneumatically powered drop-weight impact apparatus with advanced diagnostics, which we refer to as the crush gun, we can mimic conditions similar to those in the drop hammer test but with increased projectile speeds and high-speed and infrared cameras. Using these diagnostics, we analyze the formation and propagation of ignition sites that are undetectable in the standard drop hammer test. Two batches of DAAF with different particle sizes have been investigated using the drop-weight impact test and crush gun assembly, including different initial densities (pressed pellets versus free-flowing powders) and tests with and without grit particles. For the first time, this study evaluates the explosive phenomena that constitute a reaction threshold for less-sensitive explosives such as DAAF in the drop-weight impact test and how to further evaluate handling sensitivity with explosives that fall into the less-sensitive regime.

Scheme 1. Explosives DAAF (3,3′-Diamino-4,4′-azoxyfurazan) and HMX (1,3,5,7-Tetranitro-1,3,5,7-tetrazoctane)

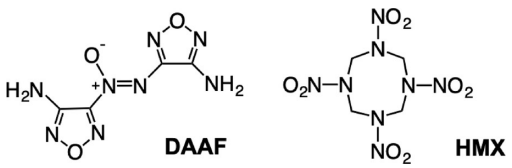

EXPERIMENTAL SECTION

Materials and Methods

All DAAF used during experimentation was synthesized using the literature-reported oxone synthesis.[47] $DAAF_C$ (coarse DAAF) was used with no further purification or particle size adjustment.[55] For the preparation of $DAAF_N$ (nanosized DAAF), a mixture of 30 g of $DAAF_C$ was suspended in 400 mL of deionized water and dispersed with an ultrasonic probe in a cylindrical flask, followed by milling in a Netzsch MiniCer bead mill for 60 min at 5500 rpm. Afterward, the slurry was loaded into a Harvest Right freeze-dryer for lyophilization in order to obtain nanometer-sized particles,[56] as particle size can be important in controlling initiation behavior inside detonators. HMX was purchased from Holston (standard MIL-DTL-4544C), dried, and used as received. Sapphire anvils were sourced from Knight Optical. ^{1}H-NMR and ^{13}C-NMR were recorded on a 400 MHz Bruker spectrometer. NMR signals were referenced using residual solvent signals.

Explosive Pressing

All explosives (DAAF and HMX) were pressed into cylindrical pellets. DAAF was pressed into pellets with a density of 1.60 g/cm^3 with the following dimensions: 4 mm diameter, 2.75 mm height, and a nominal mass of 0.055 g. HMX was pressed into pellets with the following dimensions: 4 mm diameter, 2 mm height, and a nominal mass of 0.045 g.

SEM Imaging

Scanning electron microscopy (SEM) image analyses were performed by the High Explosive Science and Technology group, Los Alamos National Laboratory (LANL). The SEM used for this work is a JEOL 7000F field emission microscope with a Schottky type (T-FE) gun with a secondary electron (SE) signal optimum resolution of ~10 nm. SEM images shown are those of the SE emission capture.

https://doi.org/10.1021/acsmaterialsau.1c00013
ACS Mater. Au 2021, 1, 116−129

Particle Size: Laser Diffraction

Explosive powders were suspended in a solution of 1% Triton X-102 in water. The suspension was inserted into an LS13 320 multi-wavelength laser diffraction particle size analyzer (Beckman Coulter Inc.) to a measured obscuration of 8−12%. All particles were sized using water as the fill medium, a 40% pump speed, and a 60 s run duration. Each lot was sampled, sized in triplicate, reported as a standard mean that was derived through the Fraunhofer theory optical model. The measurement of the light scattering pattern (collected from angles of ∼0−144°) was then translated into Heywood's diameter or the equivalent circular area diameter (ECAD), which was calculated according to ECAD = $(4A/\pi)1/2$, where A is the observed image area.[57] Note that the reported size distributions and distribution means are therefore spherical approximations regardless of their aspect ratio.[58] The instrument was checked for accuracy prior to use with Coulter size standards LS Control G15 (nominal 15 μm garnet) and LS Control GB500 (nominal 500 μm glass beads).

Drop-Weight Impact Test Setup

Drop-weight impact testing was performed with ERL type 12 drop hammer equipment using a 2.5 kg weight, a 0.8 kg striker, and sound detection equipment (Brüel & Kjaer 2238 Mediator). The striker was placed gently on top of the sample, making only minimal contact with the material before testing. For each run, 40 mg of the material was used either on grit paper or directly on the smooth (bare) anvil and impacted using the drop weight from various heights. A "go" was defined as a 117 dB average from two sound detectors, one behind the equipment and one to the left of the equipment (33 in. from the center of the microphone to the center of the anvil for both). For the measurements conducted in our laboratories, sound levels were collected for each drop. Ambient noise in the room was approximately 80 dB. The only observable in this test used to determine whether a sample has undergone reaction is crossing a sound threshold of 117 dB. During typical use of the drop weight equipment, sound levels are not recorded but rather used to determine if a reaction has occurred. However, in these studies sound data were recorded for every drop for both the DAAF and HMX samples. The parameter reported is the DH_{50}, which is defined as the height from which 50% of the drops are expected to be a "go". The drop heights used and the resulting DH_{50} values were calculated using the Neyer D-Optimal method[59] as implemented in the Neyer SenTest software. A higher DH_{50} value for an explosive correlates with a lower ignition sensitivity.

Crush Gun Apparatus and Setup

The Crush Gun is a custom-built apparatus that is essentially a pneumatically powered drop-weight tower. The barrel is ≈2 m long, with a 50.8 mm internal diameter. The projectile is comprised of the following three parts: a front impactor, a hollow body, and a back plate. All three parts were made from 17 to 4 PH stainless-steel. The summed nominal mass of the projectile assembly is 980 g. The diameter of the projectile face is 31.75 mm. The gun barrel is oriented vertically, with the breech at the top, and bolted to a vacuum chamber. In order to prevent an air pulse from traveling down the barrel ahead of the projectile and disturbing the sample before impact, a rough vacuum (≈3 Torr) was applied to the chamber prior to firing. Two Viton o-rings seal the projectile inside the barrel. A remotely operated pneumatic actuator prevents the projectile from moving down the barrel as the vacuum is pulled on the chamber. The chamber above the projectile (breech) is pressurized between 0 and 60 psi with an inert gas to force the projectile down the chamber at the sample. The speed of the projectile can be determined using video imaging of the high-speed cameras used to determine the projectile's change in position per unit of time. A schematic of the crush gun apparatus can be seen below in Figure 1.

The sample is placed on a sapphire anvil (63.5 mm diameter) and centered using a plastic jig (pellets fit into the center of the jig, while powder is added to the center of the jig and centered with a spatula once the jig is removed). During testing, the projectile impacts the sapphire anvil, shattering it. A mirror is present for imaging, which generally does not shatter. Triggering is accomplished with a piezo pin

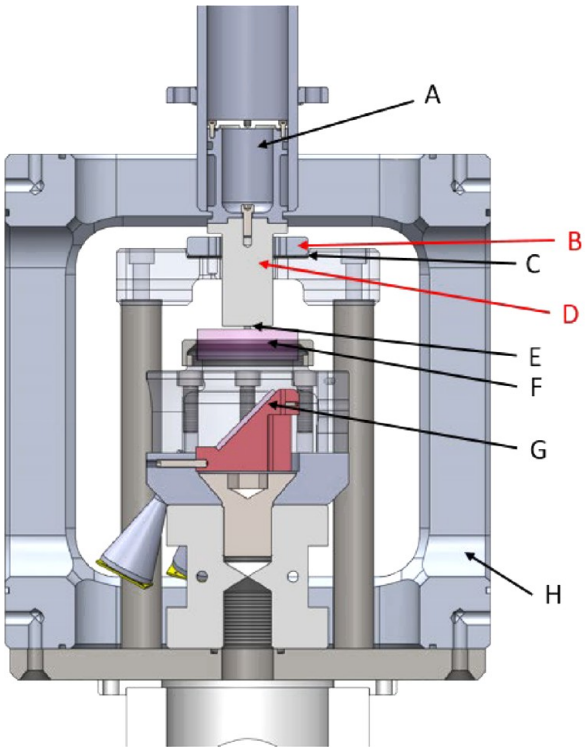

Figure 1. Schematic of the crush gun firing chamber. (A) Projectile body; (B) stop pad; (C) 1.6 mm thick rubber pad, laser cut, to help arrest the projectile gently; (D) projectile impactor; (E) the explosive pellet shown is 4 mm in diameter and 2 mm in height; (F) sapphire window for high-speed imaging (and strength); (G) turning mirror for high-speed imaging; and (H) vacuum chamber.

spaced off the anvil before each test such that the shoulder of the projectile impacts the pin at a controlled height above the anvil surface. For solid pellet samples, the sample itself is used to control the height of the trigger pin so that time zero coincides with the first sample contact. The physical precision of the pin spacing is ≈0.03 mm; error in the trigger timing is dependent on the projectile velocity.

High-speed cameras view the reaction through transparent sapphire windows. Two visible light Phantom V2512 cameras are employed for simultaneous bottom and side views. The high-speed cameras with the bottom views, which were used in this work, were set to a 7.23 μs exposure time, with 130,000 frames per second (7.69 μs). In these settings, 0.46 μs is not recorded between frames. The projectile impact velocity is obtained by image analysis of the side-view visible camera, which was captured at 110 000 fps. A FLIR X6901sc infrared camera (3−5 μm nominal sensor response) captures the bottom view. A 50/50 polka-dot aluminum beam splitter and a silvered turning mirror provide the visual and infrared cameras simultaneous access to the bottom view. To capture low-temperature phenomena (and to "freeze" the motion), extremely short integration times were used. Sensor counts were often close to the noise floor, and the sensor response in this regime is nonlinear. Thermography calibration was performed in situ through all intervening optical elements using area and cavity blackbody sources. At the frame dimensions required to spatially resolve reaction details, the minimum integration time of the FLIR is ≈0.5 μs (which provides adequate temporal resolution), while the minimum interframe time is ≈100 μs (which provides inadequate temporal resolution). The video functionality is therefore too slow to record a video record of a single event. This limitation of the infrared camera allows only a single image to be captured from each test. The evolution of the explosive reaction is therefore constructed from single images collected at different moments from an ensemble of nominally identical tests.

Grit used in the crush gun testing was either 150 grit paper or sand. The sand is a high-quality commercially available silica sand product

https://doi.org/10.1021/acsmaterialsau.1c00013
ACS Mater. Au 2021, 1, 116−129

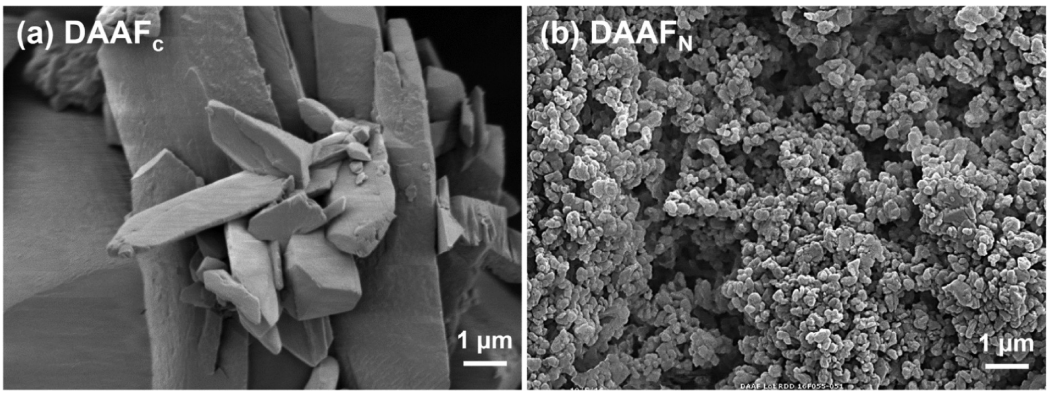

Figure 2. SEM images of DAAF with a 1 μm scale bar. (a) DAAF$_c$ and (b) DAAF$_N$.

(federal fine grade, U.S. Silica Company, PO Box 577, Ottawa, IL) mined from the St. Peter Sandstone formation near Ottawa, IL. To control the grit diameter, the sand was initially sorted into 250−500 μm size fractions using ASTM E11 U.S. standard test sieves (Precision EForming, LLC, Cortland, NY 13045) and then individual grains were selected by hand using a Keyence VHX-600 digital microscope.

RESULTS AND DISCUSSION

Particle Size Analysis

Two batches of DAAF with different particle sizes have been prepared for this study, i.e., nanosized DAAF (DAAF$_N$) and coarse DAAF (DAAF$_C$), Scanning electron microscopy for DAAF$_N$ and DAAF$_C$ was conducted to analyze the particle size and morphology of the materials (Figure 2). SEM imaging of the two samples of DAAF show that DAAF$_C$ has larger particle sizes, with crystals approximately 40−50 μm long, while DAAF$_N$ particles are uniform and much smaller compared to those of DAAF$_C$, with a particle size range of 100−500 nm. Coulter particle size analysis (PSA) was also performed for DAAF$_C$ (Table 1), which was consistent with the SEM imaging. DAAF$_N$ was analyzed using the Coulter analysis, but because nanosized particles tend to form agglomerates when wet the measured values for particle size are artificially large. The mean particle sizes of the different HMX classes varied from 34.72 to 1025 μm (Table 1). The classes of HMX have well-defined size constraints (MIL-DTL-45444C), which relate to what percentage will fit through what size screen. Class II appears particularly fine in comparison to the sieve requirements, where 75% should fit through a 45 μm sieve. SEM images of the four classes of HMX can be seen in Figure 3.

Table 1. Particle Size Measurements (Coulter PSA) for HMX and DAAF (μm)

material	mean	median (<50%)	<90%	<10%
DAAF$_C$	87.00	56.02	218.8	2.183
DAAF$_N$	52.05	41.59	114.8	4.414
HMX class I	203.3	169.0	364.4	66.78
HMX class II	23.05	6.163	80.79	1.844
HMX class IV	1025	956.4	1559	642.2
HMX class V	34.72	12.25	103.8	1.808

Drop-Weight Impact Tests

Previous drop-weight impact test results with DAAF have indicated that the explosive is quite insensitive to a nonshock-induced impact, with drop heights at the upper limit of the test (>320 cm).[52] However, in recent drop-weight testing by the authors, DAAF exhibited DH$_{50}$ values (the height from which 50% of the drops exhibited an audible "go") at significantly lower values than those previously recorded.[6] Higher DH$_{50}$ values correspond to more energy required to generate a reaction, or "go", using sound meters. To address the discrepancy, we have examined the impact sensitivities of DAAF$_N$ and DAAF$_C$ both with and without grit paper. DH$_{50}$ values for both batches of DAAF were lower than 320 cm (Table 2), with values of 263.2 ± 69.6 cm for DAAF$_N$ and 292.6 ± 34.4 cm for DAAF$_C$; both had very large standard deviations. The DH$_{50}$ value for DAAF$_N$ with finer grit sandpaper (1200 grit) was within the error of the value obtained with the standard coarse sandpaper (150 grit). When no grit paper was used (DAAF$_N$ and DAAF$_C$ on a bare anvil), the DH$_{50}$ values were significantly lower at 119.2 ± 3.8 cm and 123.7 ± 3.4 cm, respectively. Though the DH$_{50}$ values did not vary significantly with particle size or the grit paper type, the drop heights were lower in the absence of grit paper, which was surprising given that grit is typically regarded as a sensitizer.

It should be noted that DAAF samples ran in the cases of both grit and no grit were audibly loud enough (117 dB) to be considered a "go"; however, in all cases it appeared that most of the material remained after each drop, which was not necessarily unexpected with a very insensitive explosive. The residual material leftover after each drop was a light brown color, slightly darker than the original orange color of the DAAF. However, NMR spectroscopy indicated no change in the material after impact (Figure 4), suggesting that any chemical decomposition was <1% (likely a small percentage of highly colored impurities) that we would not expect to influence sensitivity testing results.

Owing to the unexpected results with DAAF, a more sensitive material, HMX, was chosen for comparison. Four types of HMX (class I, class II, class IV, and class V) with different particle size distributions were tested for impact sensitivity (Table 2). The measured values were consistent within error across all four classes of HMX despite the significant differences in particle size. DH$_{50}$ values for the four HMX classes ranged from 18.9 ± 5.8 to 29.5 ± 2.7 cm, with no observable correlation with the particle size. Drop-weight impact testing without grit on the bare anvil showed almost no change in DH$_{50}$ values for the four HMX classes (Table 2). In contrast, we have observed that DH$_{50}$ values for PETN and other standard explosives typically increase on the bare anvil relative to the values collected using grit.[6,60]

https://doi.org/10.1021/acsmaterialsau.1c00013
ACS Mater. Au 2021, 1, 116−129

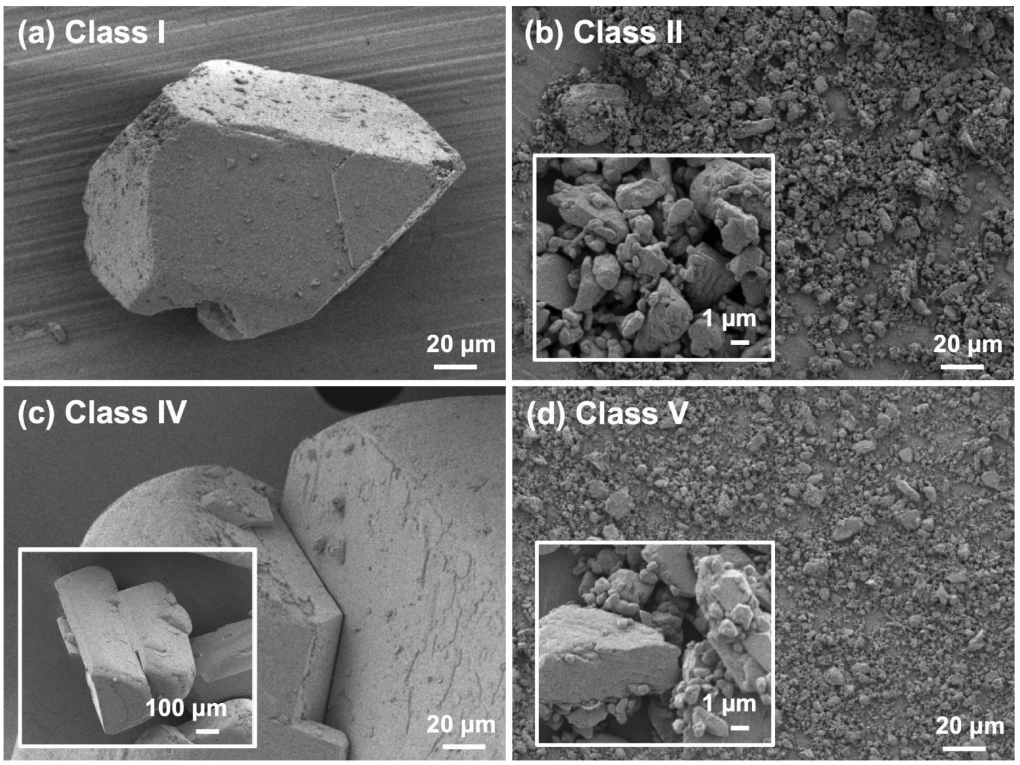

Figure 3. SEM images for (a) class I, (b) class II, (c) class IV, and (d) class V HMX.

Table 2. Drop-Weight Impact Test Results for DAAF Samples, PETN, and HMX

material (conditions)[a]	impact D_{H50} (cm) *with grit*	impact D_{H50} (J) *with grit*	impact D_{H50} (cm) *bare anvil*	impact D_{H50} (J) *bare anvil*
$DAAF_N$	263.2 ± 69.6	64.5 ± 17.1	119.2 ± 3.8	27.4 ± 0.86
$DAAF_N$ (1200)	222.0 ± 42.4	54.4 ± 10.4		
$DAAF_C$	292.6 ± 34.4	71.8 ± 8.4	123.7 ± 3.4	30.3 ± 0.8
HMX class I	18.9 ± 5.8	4.6 ± 1.4	24.9 ± 15.0	6.1 ± 3.7
HMX class II	23.2 ± 1.3	5.7 ± 0.32	26.0 ± 4.9	6.4 ± 1.2
HMX class IV	29.5 ± 2.7	7.2 ± 0.66	27.6 ± 1.0	6.8 ± 0.25
HMX class V	25.2 ± 2.7	6.2 ± 0.65	29.0 ± 2.1	7.1 ± 0.51
PETN	12.3 ± 2.2	3.0 ± 0.54	21.4 ± 2.1	5.2 ± 0.51

[a]Except for $DAAF_N$ (1200 grit), 150 grit was used for all samples.

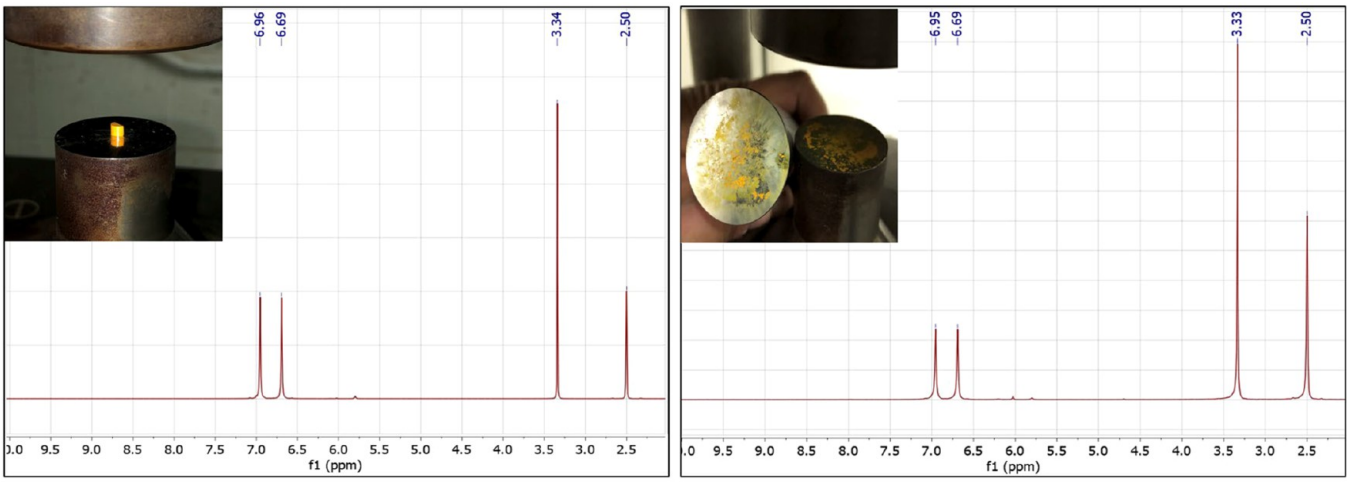

Figure 4. NMR spectroscopy. (Left) $DAAF_N$ pellet (broken in order to reduce the mass to a typical 40 mg sample size). NMR was run in d_6-DMSO (2.5 ppm), and water was observed in the sample (3.33 ppm). (Right) After impact from a drop height of 320 cm, no grit, decibel level not recorded. NMR was run in d_6-DMSO (2.5 ppm), and water was observed in the sample (3.33 ppm).

https://doi.org/10.1021/acsmaterialsau.1c00013
ACS Mater. Au 2021, 1, 116−129

Sound level data for each impact test drop of DAAF and HMX can be seen in Table 3 and Figure 5, where the sound

Table 3. Sound Levels for DAAF, PETN, and HMX

material (conditions)[a]	sound level average (dB) for a "go" *with grit*	sound level average (dB) for a "go" *bare anvil*	sound level average (dB) for a "no go" *with grit*	sound level average (dB) for a "no go" *bare anvil*
$DAAF_N$	121 ± 3	122 ± 3	111 ± 2	108 ± 2
$DAAF_N$ (1200)	120 ± 3	122 ± 3	111 ± 2	108 ± 2
$DAAF_C$	120 ± 3	122 ± 4	113 ± 4	110 ± 4
HMX class I	123 ± 3	126 ± 4	99 ± 7	100 ± 5
HMX class II	123 ± 3	128 ± 4	98 ± 2	100 ± 7
HMX class IV	129 ± 4	128 ± 3	99 ± 2	100 ± 4
HMX class V	126 ± 5	126 ± 4	99 ± 2	102 ± 8
PETN	129 ± 2	130 ± 3	98 ± 6	100 ± 5

[a]Except for $DAAF_N$ (1200 grit), 150 grit was used for all samples.

threshold for a "go" is represented by the horizontal lines in each plot. The plots with HMX have a clearly defined separation between a "go" (above 117 dB) and a "no go" (well below 117 dB) with better separation apparent in the grit-containing samples, likely due to reliable sources of ignition through friction in those samples. This "S-shaped" curve is the expected behavior in a drop-weight impact test with a mostly unambiguous initiation for a more sensitive explosive.[28] In contrast, the DAAF samples have a narrower distribution of sound levels around the 117 dB threshold. The average sound level for a "go" for all DAAF samples was 121 dB, and the average level for a "no go" was 111 dB (Table 3), with a difference of 10 dB between the average "go" and "no go". In contrast, the average "go" level was 126 dB for all HMX samples, and the average "no go" level was 100 dB, giving a much larger and unambiguous separation of 26 dB.

In less-sensitive explosives (such as DAAF), the increased height from which the striker is dropped will generate more noise than the lower drops required for sensitive explosives (like HMX). In order to show how sound levels vary with drop height in the absence of violent reactions, Figure 5 also includes sound levels collected for two inert materials, namely, erythritol sugar (coarse grains) and fine icing sugar (fine particles), over a range of 5−320 cm. For the drops in the presence of grit, sound levels remained at or under 110 dB, lower than the established threshold of 117 dB. Inert samples run on the bare anvil showed slightly increased sound levels when compared to those of the grit samples, possibly due to the lack of a "cushioning" effect created by the grit paper. It should be noted that samples of icing sugar on the bare anvil exhibited a large amount of scatter between 110−120 dB at drop heights >110 cm, with even one "go" at just above the sound level threshold.

Due to the large scatter observed in the collected sound data for the different samples of DAAF (Figure 5b), it is possible that small adjustments in the threshold for a "go" could substantially affect the calculated DH_{50} value. In contrast, a very clear separation was observed in HMX samples between "go" and "no go" values (Figure 5a), following the expected "S-curve" behavior.[28] Removing the grit paper resulted in lower DH_{50} values (higher sensitivity) for both particle sizes of DAAF, which was unexpected since we had removed a reliable source of ignition (Figure 5e). This may be due an artifact with

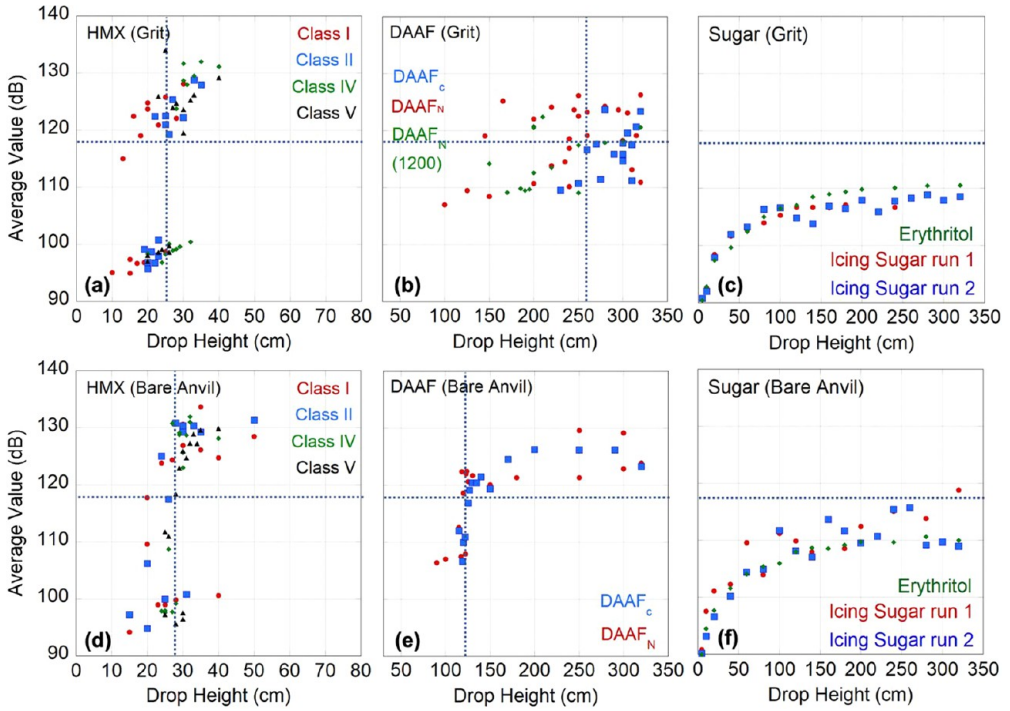

Figure 5. Average sound level from two sound meters (dB) versus the drop-weight impact height (cm) for (a) HMX class I, II, IV, and V with grit present; (b) $DAAF_c$ and $DAAF_N$ with grit present; (c) inert erythritol (coarse) and icing sugar (fine) with grit present; (d) HMX class I, II, IV, and V on the bare anvil; (e) $DAAF_c$ and $DAAF_N$ on the bare anvil; and (f) inert erythritol and icing sugar on the bare anvil. Horizontal dotted lines are drawn at the the 117 dB "go"/"no go" threshold, and vertical lines show the calculated impact sensitivity value after the statistical analysis. Note that the *y*-axes for all plots are the same but the *x*-axes for DAAF and HMX are enlarged to the area of interest.

https://doi.org/10.1021/acsmaterialsau.1c00013
ACS Mater. Au 2021, 1, 116−129

sound collection rather than some inherent property of the material. This is supported when looking at the sugar control runs in Figure 5c versus Figure 5f in which the sound levels for the bare anvil are larger than the corresponding values when grit is used. Additionally, the scatter observed in the dB levels for DAAF samples on the bare anvil at >150 cm (Figure 5e) is also observed in the inert samples on the bare anvil (Figure 5f). It is important to note that the Neyer deoptimal method of establishing DH_{50} standard deviations accounts for scatter in the data; however, it does not account for variation in dB levels as you increase the drop height. Though the drop-weight impact test is useful for determining whether a novel energetic is safe to handle, it was not intended for meaningful or reproducible rankings of less-sensitive explosives (>150 cm). This becomes especially difficult when sound level data exhibit a large amount of scatter within a narrow range of values (i.e., 10−15 dB). In order to probe the ignition and propagation behavior for DAAF, more advanced visible diagnostics are required.

Crush Gun Tests

The crush gun uses pressurized air to propel a ∼980 g projectile down a ∼2 m vertical barrel. The explosive sample rests on a sapphire anvil inside a sealed chamber, which is evacuated prior to testing to eliminate the air pulse ahead of the projectile that would otherwise disturb the sample. The sapphire anvil permits diagnostic imaging of both the side and bottom of the explosive during testing. Glass anvils have been used as early as the 1950's and are necessary to visually detect the formation of ignition sites during a nonshock impact event.[61] Ignition sites have been observed in previous studies with HMX and PETN using impact-type testing with glass anvils, which were speculated to be initiated by void collapse and adiabatic shear-band mechanisms.[62−66] Additional studies have looked at the effect of grit on HMX-PBX formulations during nonshock impact studies.[67] In the absence of added grit, reactions that lead to ignition site formation are commonly observed in regions of intense localized plastic shear[68−70] rather than through heat induced by friction from a source of high-melting-point grit. Using this apparatus allows for both high speed and infrared imaging of the sample during the impact event, allowing us to see the ignition and propagation of any thermal events. For the purpose of this study, we define explosive ignition as the onset of luminous exothermic gas-phase reactions and post-ignition propagation as deflagration that is sustained through the material.

It should be noted that though both the drop-weight impact test and crush gun both evaluate sub-shock ignition, the impact dynamics are quite different. Therefore, comparisons between the experiments are necessarily qualitative. The mass of the crush gun impactor is lower than that of the drop-weight (980 versus 2500 g, respectively), so the ratio of the kinetic impact energy to the momentum is higher for the crush gun. Additionally, the maximum amount of available kinetic energy at the moment of impact in the drop-weight test (at 320 cm, with a 2.5 kg drop weight and a velocity of 7.9 m/s) is approximately 78 J. In contrast, the available kinetic energy at the highest projectile speed (32.5 m/s) using the crush gun in these experiments is approximately 518 J, a factor of seven higher in energy than what would be present at the highest setting in the drop-weight test. The lowest projectile speed of 11.1 m/s in the crush gun would have an energy of 60 J, which would correspond to a 245 cm drop height on the impact test instrument (this is close to the average DH_{50} value for the DAAF samples tested with grit, Table 2). Finally, the material properties of the projectile and the anvil affect the fraction of kinetic energy that is transferred into the elastic deformation of those components during the impact (rather than the dissipative heating of the sample) and is therefore an influential factor in the drop-weight behavior.[28]

For the crush gun tests, $DAAF_N$ was pressed into pellets with dimensions of roughly 4.0 mm diameter and 2.75 mm height and a mass of 0.055 g. Pellets were loaded into a firing chamber that was then evacuated to eliminate movement of the sample as the projectile was dropped, and the projectile propellant pressure was varied to control the impact velocity. $DAAF_N$ pellets were impacted with projectiles fired at speeds between 11.1 and 32.5 m/s (Table 4). High-speed imaging was used to view the powder as it crushed and spread during the test, and visible light was generated for tests performed above 19 m/s (Figure 6). In all cases, visible sites were observed along the outer edge of the material where the explosive powder was at its thinnest (vanishing thickness). Studies conducted by Kennedy[35] showed that when crushing an explosive the highest radial velocities occur at the outer edge of the material and suggested that high internal velocity gradients drove the visco-plastic heating that led to ignition.

Table 4. Crush Gun shots of $DAAF_N$ Pellets, $DAAF_N$, and $DAAF_C$ Powder

explosive (shot number)	pellet or powder	breech pressure (PSI)	projectile speed (m/s)	grit	ignition sites visible
$DAAF_N$ (88)	pellet	60	32.5	no	yes
$DAAF_N$ (90)	pellet	40	28.8	no	yes
$DAAF_N$ (91)	pellet	20	21.4	no	yes
$DAAF_N$ (94)	pellet	20	21.4	no	yes
$DAAF_N$ (93)	pellet	15	19.0	no	yes
$DAAF_N$ (98)	pellet	15	19.0	no	no
$DAAF_N$ (92)	pellet	10	16.6	no	no
$DAAF_N$ (104)	powder	20	21.4	no	yes
$DAAF_N$ (105)	powder	15	19.0	no	yes
$DAAF_N$ (106)	powder	10	16.6	no	no
$DAAF_N$ (112)	powder	0	11.1	*yes*[a]	yes
$DAAF_N$ (113)	powder	40	28.8	*yes*[b]	yes
$DAAF_C$ (95)	pellet	40	28.8	no	yes
$DAAF_C$ (96)	pellet	20	21.4	no	yes
$DAAF_C$ (97)	pellet	15	19.0	no	yes
$DAAF_C$ (107)	powder	20	21.4	no	yes
$DAAF_C$ (108)	powder	15	19.0	no	yes
$DAAF_C$ (109)	powder	10	16.6	no	no
$DAAF_C$ (110)	powder	10	16.6	*yes*[a]	yes
$DAAF_C$ (111)	powder	0	11.1	*yes*[a]	yes
HMX (100)	pellet	0	11.1	no	yes[c]

[a]A single grain of sand was placed in the center of the sample. [b]Sandpaper was used as the source of grit. [c]Propagation was observed on the timescale of the test with this sample.

https://doi.org/10.1021/acsmaterialsau.1c00013
ACS Mater. Au 2021, 1, 116−129

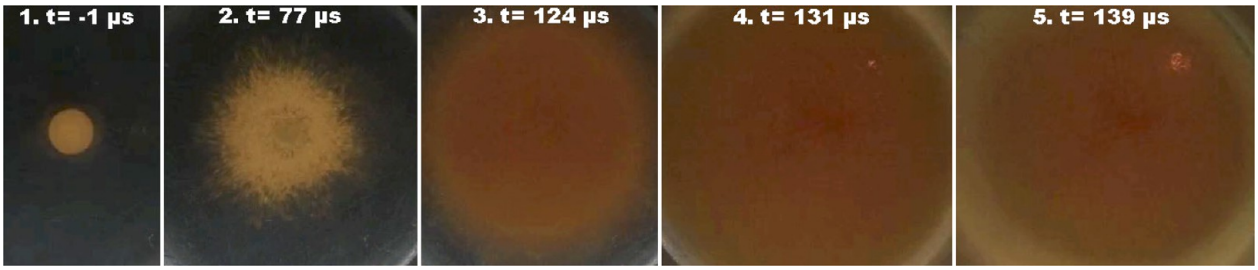

Figure 6. Crush gun shot of a $DAAF_N$ pellet with projectile speed of 21.4 m/s. Frame 5 is the last recorded frame before the sapphire window broke. Time is relative to the trigger location, which cannot be correlated to an absolute event.

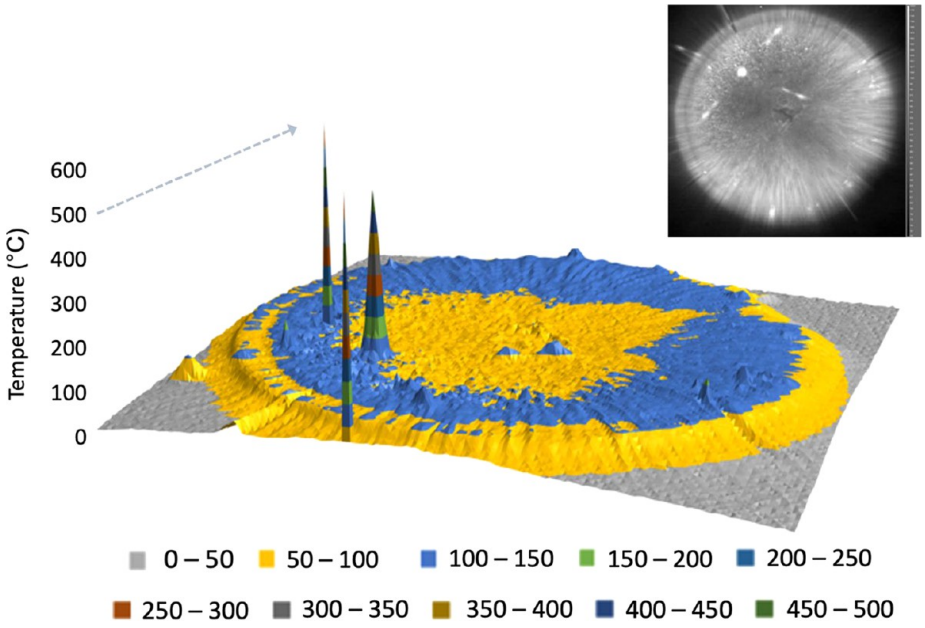

Figure 7. IR temperature surface plot and image (inset) for a $DAAF_N$ pellet tested at 21.4 m/s (test 91), showing three ignition sites approaching 500 °C. The four-component "star" pattern of light is caused by an optical element (50/50 beam splitter) and does not portray the explosive response, so the center peak is the only "real" hotspot.

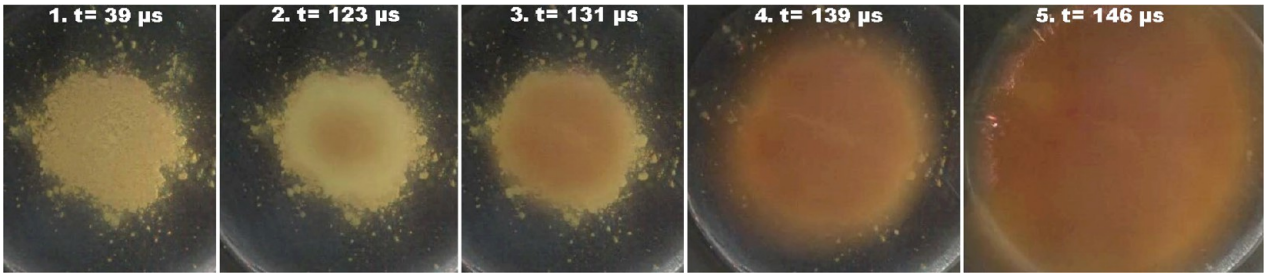

Figure 8. Crush gun shot of the $DAAF_N$ powder with a projectile speed of 21.4 m/s. Frame 5 is the second-to-last recorded frame before the sapphire window broke.

Figure 6 shows camera frames of a $DAAF_N$ pellet shot at 21.4 m/s as it was crushed. The first frame shows the pellet prior to contact with the projectile. During the second frame, a faint increase in brightness can be observed as the sample power is pressed against the anvil.[71] However, additional compression darkens the material to a reddish hue (observed in all DAAF shots). The cause of this darkening remains unknown. Rubblization of the $DAAF_N$ is visible in frame 4 and is more visible at the slower firing speed. Frame 5 shows the formation of a single ignition point that is visible in the top right of the material; this is the last frame before the sapphire breaks from the projectile impact. IR camera frames (Figure 7) taken during this test show heating throughout the sample, with the hotter regions on the outer edge of the explosive. The visible spot in Figure 7 in the top left of the IR image (inverted due to the mirrors used) is the hottest point on the image, confirming it is due to the high explosive heating that is expected in an ignition site. Ignition sites observed during these tests reach a minimum of 500 °C due to temporal blur, spatial resolution, and sensor saturation, though they are expected to be much hotter. It is important to note that ignition sites that formed on the top surface would be hidden from view in this setup.

https://doi.org/10.1021/acsmaterialsau.1c00013
ACS Mater. Au 2021, 1, 116–129

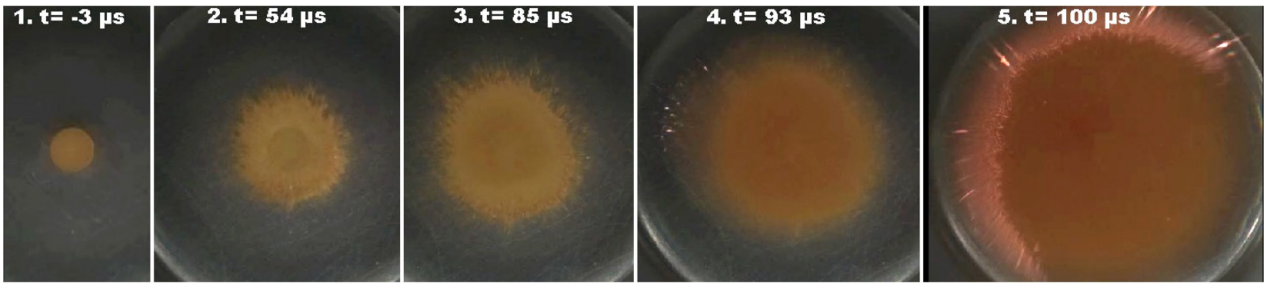

Figure 9. Crush gun shot of a $DAAF_N$ pellet with a projectile speed of 28.8 m/s. Frame 5 is the second-to-last recorded frame before the sapphire window broke.

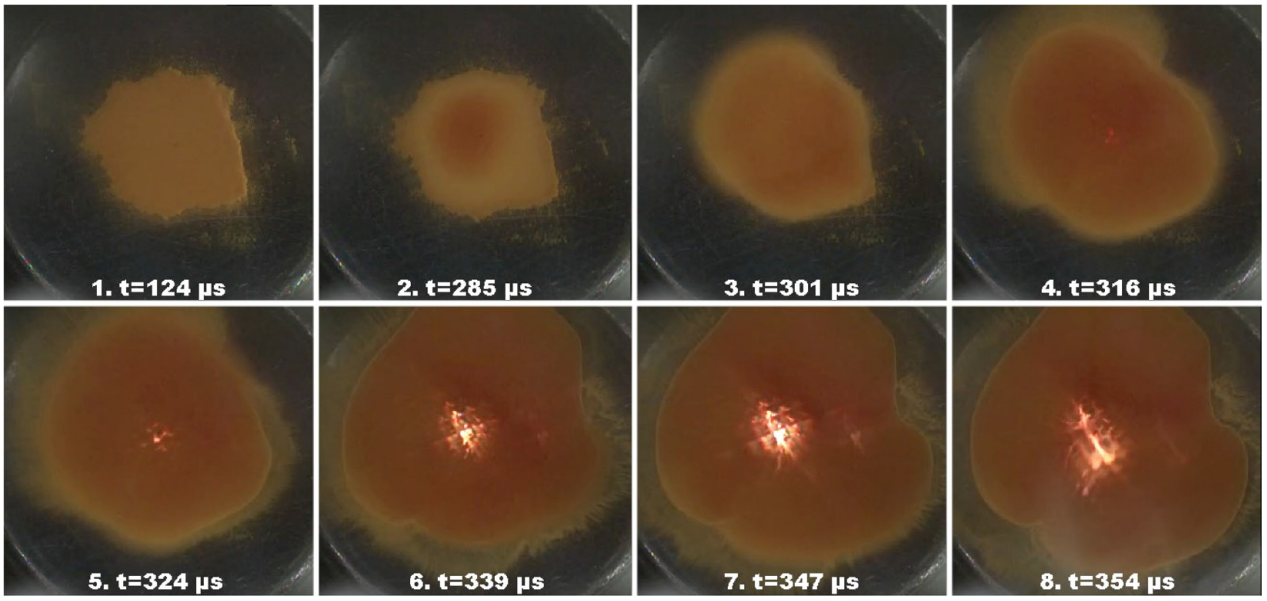

Figure 10. Crush gun shot of $DAAF_c$ powder with added grit particles. The projectile was not pressurized, and the velocity was 11.1 m/s (0 psi). Frame 8 is the second-to-last recorded frame before the sapphire window broke.

No ignition site was formed in any shot of $DAAF_N$ prior to the rubblization of the material. After the material was compressed, the originally consolidated pellet was thoroughly rubblized and superficially resembled a powder sample. Due to this observation, it was hypothesized that $DAAF_N$ pellets would react similarly to $DAAF_N$ powder. Figures 6 and 8 compare the results of the representative tests of $DAAF_N$ pellets and the powder, respectively, fired with projectile speeds of 21.4 m/s. Both show the formation of ignition sites on the outer edge of the material. Overall, the results appear to be the same between the pellets and powder of the same material, though more data would be needed for a statistically significant comparison.

Figure 9 shows still images from a $DAAF_N$ pellet impacted with a projectile at a higher impact velocity of 28.8 m/s. In frame 5 (the final frame before the sapphire shattered), visible light encompasses one-half of the outer edge of the material, which is consistent with the increased radial velocity contributing to ignition site formation. Ignition sites were observed in the $DAAF_N$ powder and pellets at 19.0, 21.4, 28.8, and 32.5 m/s projectile speeds but not at 11.1 and 16.6 m/s projectile speeds, giving an approximate threshold impact velocity for the formation of ignition sites of ~19.0 m/s. More analyses would be required to determine a statistically significant threshold. For all videos, there was an interframe time of 7.69 μs, including a 7.23 μs exposure time, meaning that only 0.46 μs was not recorded. Any bright hotspot would likely be captured in these conditions, up until the sapphire window breaks. Despite the visual presence of ignition sites observed in $DAAF_N$ pellets and powder samples at multiple firing pressures, no propagation of those sites into a deflagration event was observed in any of the shots during the time scale of the tests.

$DAAF_C$ powder was also analyzed at projectile speeds of 16.6, 19.0, and 21.4 m/s. Ignition sites for $DAAF_C$ were observed in all shots of 19.0 m/s and greater, and no ignition sites were observed at 16.6 m/s, which is consistent with the behavior observed for $DAAF_N$. Just as in all previous cases with $DAAF_N$, no propagation toward a deflagration event was observed in the $DAAF_C$ powder despite the formation of ignition sites.

In order to analyze the effect of grit during the crush gun experiments, small-particle-size grit (500 ± 250 μm longest dimension) was placed within the explosive powder prior to firing. The grit chosen is over 99% pure quartz with well-rounded edges, making it relatively strong under compressive loading and ideal for the crush gun shots. Figure 10 shows still frames from the high-speed camera of a shot conducted on $DAAF_C$ at a 11.1 m/s projectile velocity, with a single grain of sand placed in the center of the pile. Figure 11 shows two grains of sand on a piece of the drop-weight impact test standard grit paper for a grain size comparison. This image also

https://doi.org/10.1021/acsmaterialsau.1c00013
ACS Mater. Au 2021, 1, 116–129

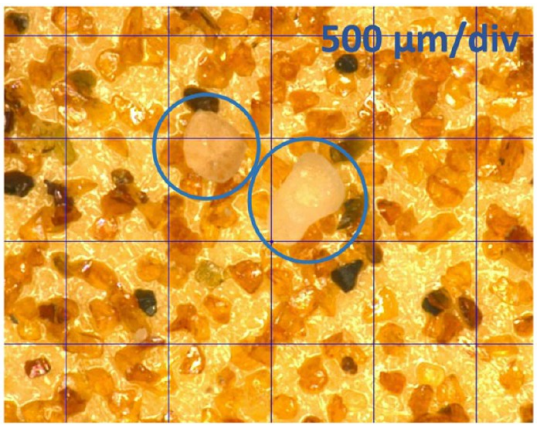

Figure 11. Micrograph of two pieces of loose grit (white pieces, top-center, circled) resting atop standard drop-weight impact test grit paper. Notice that the grit particles in the sandpaper are reddish—likely garnet—and smaller than the grit that was hand-selected for the loose grit experiments. The image was taken at 500 μm/division.

illustrates the difference between loose grains of sand and grit paper, as the adhesive bonding grains to the grit paper is visible beneath and covering the grit particles. Similar to the previous shots, as the material is compressed, the color changes to a reddish hue. Light generated from the ignition site begins to become visible in frame 4 at the center of the pile of the explosive, where the grit particle was placed. The ignition site is at the center of the explosive, which is in contrast to previous shots where ignition sites formed at the outer edge of the material. This is due to the heating of the HE that is in contact with the hot grit particle on the sapphire. Identical shots were conducted with projectile speeds of 11.1 m/s both with $DAAF_N$ and with $DAAF_C$, and each showed ignition sites where the grit was placed. No propagation to a deflagration event was observed in any shot with a DAAF sample, either with or without grit particles present. It is important to note the location of the ignition sites in the tests using grit. In the absence of grit particles, we only observe ignition sites at the edges, which is consistent with either increased shear banding (fastest moving at the edges) or anvil deformation (potential pinching of the explosive at the edges). In the presence of grit, the formation of ignition sites occurs at the lowest projectile speeds, with single grit particles, and only in the location of the placed grit.

In order to mimic the conditions of the drop-hammer test, sand paper (120 grit, Figure 11; a commonly used grit in drop-hammer tests) was adhered to the face of the projectile. This shot (shot 113, Table 4) was conducted with $DAAF_N$ powder and a 28.8 m/s projectile velocity. Still frames are shown in Figure 12, where ignition sites can be seen at the perimeter of the explosive material as well as in the center. The ignition sites are more delocalized in this experiment due to the presence of hundreds of grains of evenly dispersed high-melting point grit (rather than 1 or 2 grains of sand placed in the center of the sample).[72] Again, no propagation of any ignition site was observed during the time scale of this test (<400 μs). However, the sapphire anvil shattered immediately after frame 4, so it was not possible to see if propagation would have occurred in a different test or setup. We are therefore limited in the upper limit of energy transfer to the explosive by the strength of the sapphire anvil. Because more ignition sites were observed *with* sandpaper at 28.8 m/s (Figure 12) than *without* sandpaper (Figure 9), this result does support that the presence of the sandpaper (grit) aids in the formation of ignition sites, as has been suggested in the past for drop-weight impact testing and other subshock testing.[42,43]

Just as in the drop-hammer test, a more sensitive explosive HMX (class 1) was examined with the crush gun to observe any differences when compared to DAAF. Pellets of HMX (4 mm diameter, 2 mm height, and 0.045 g) were prepared and tested in the same manner as the DAAF pellets. As HMX is considerably more sensitive than DAAF, the initial tests were conducted at the slowest projectile speed of 11.1 m/s (Figure 13). Similar to the DAAF pellets, HMX displayed ignition sites during the test that can first be observed in frame 2 of Figure 13 after considerable crushing of the sample has occurred. These ignition sites progress to a propagating deflagration event that consumes most of the explosive (frames 3 and 4). In the final frame, frame 5, the reaction has passed the most violent point and can be seen decelerating in violence. As a deflagration event was observed at the slowest possible speed, no additional tests were conducted. The shape on the anvil in the last frame is compressed and unreacted HMX, which was adhered to the sapphire post-test. The compressed HMX behaves like a consolidated explosive, which is less amenable to propagating deflagration due to reduced surface area and allows for gases to escape in the surrounding area.

Drop-weight impact test results and sound data for the HMX samples discussed previously show there is a significant difference between what is considered a "go" or a "no go", and a full reaction is visible in the lowest imparted energy in the crush gun experiments. Even at the lowest projectile speed attainable by the crush gun, HMX was observed to form ignition points that easily transitioned to a deflagration event. Despite much higher projectile speeds and the addition of grit

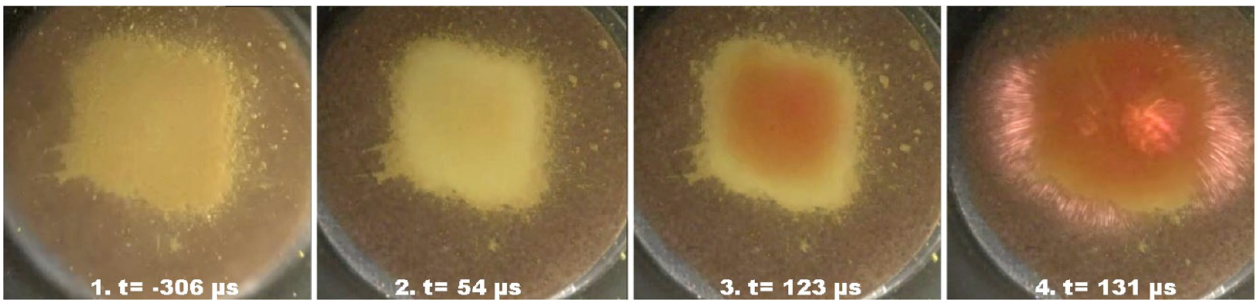

Figure 12. Crush gun shot of $DAAF_N$ powder with sandpaper adhered to the projectile face at a projectile speed of 28.8 m/s. Frame 4 is the last recorded frame before the sapphire window broke.

https://doi.org/10.1021/acsmaterialsau.1c00013
ACS Mater. Au 2021, 1, 116–129

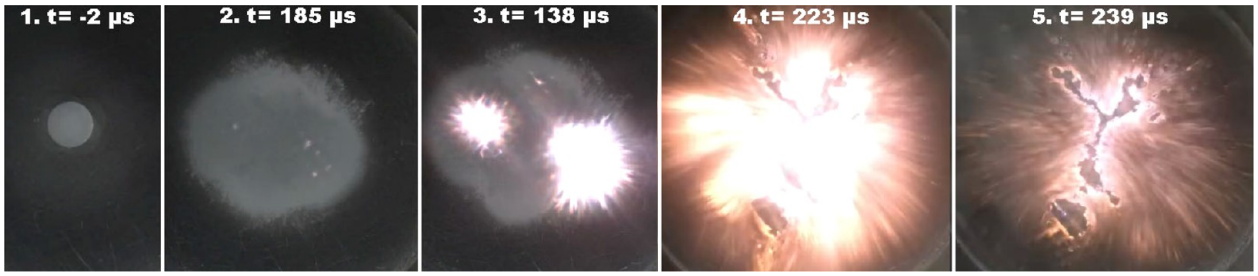

Figure 13. Crush gun shot of the HMX pellet at the slowest projectile speed of 11.1 m/s. Frame 4 is the last recorded frame before the sapphire window broke.

sources in the crush gun experiments, no DAAF sample underwent a transition from an ignition site to deflagration on the time scale of the tests. The crush gun results indicate that even under projectile velocities of 32.5 m/s (with an impact energy of 518 J), DAAF does not propagate a reaction from visible ignition sites.

When grit was present, we observed an apparent "desensitizing" effect on DAAF in the drop-weight impact test, in contrast to the crush gun where we observed the formation of more ignition sites. We believe that the discrepancy in these results may be in part due to the sound level diagnostics used in the impact test. In the drop-weight impact test, the sample must generate >117 dB in order to be considered a "go". The DAAF samples containing grit exhibited more scatter in the sound data and additionally generated overall lower dB levels (Figure 5), which is consistent with the "cushioning" effect of grit paper that was observed with the inert samples. It may therefore have been more likely for some DAAF grit samples to record a "no go" close to the threshold of 117 dB, whereas in the absence of grit paper that same reaction may have been loud enough to cross the threshold of 117 dB. The crush gun, which avoids sound thresholds, allowed us to observe ignition sites rather than infer that they occurred through sound levels.

In general, the drop-weight impact test, which is dependent on audible reports, gives a conservative estimate of the initiation behavior, i.e., ignition, with or without full propagation. This is a strength of the test because initiation can cause more violent reactions depending on the configuration of the material being tested. Though the crush gun is not a direct comparison with the drop-weight test, it does allow for visible diagnostics during the subshock impact in order to probe ignition and propagation events that otherwise cannot be separately observed using the drop-weight test.

CONCLUSIONS

Drop-weight impact tests and crush gun analyses of both DAAF and HMX of multiple particle sizes were conducted in order to study the handling sensitivity and explosive response of the materials. For the drop-weight impact tests with DAAF, the material consistently remained on the anvil even after the individual drops were determined to be "go" events. Neither particle size nor grit paper significantly influenced the results of the test, and surprisingly the DH_{50} values decreased (the handling sensitivity increased) when samples were tested on the bare anvil. These observations could be due to artifacts present in the sound collection. In contrast, HMX samples exhibited consistent DH_{50} values with low standard deviations, which did not change in the presence of grit paper versus the bare anvil. In order to better interpret the drop hammer test results, sound data were collected and analyzed for each material tested. HMX displayed clear delineations between a "go" and a "no go", most notably when examining sound data recorded during testing, exhibiting an "S-shaped" curve that was expected for standard impact tests. However, DAAF exhibited significant scatter in sound levels measured in drop-weight impact testing, with large standard deviations in the DH_{50} values. It is important to note that drop-weight impact experiments are small lab-scale tests designed to give rapid and preliminary information on the safety of an explosive (whether or not it is "safe to handle") in contrast to typically larger-scale tests that can provide more quantitative information on the specific aspects of ignition and propagation.

Using the crush gun apparatus, high-speed imaging was used to identify the formation of ignition sites in both DAAF and HMX. Two particle sizes of the DAAF material ($DAAF_N$ and $DAAF_C$) were studied and showed no difference in reactivity under these conditions. The presence of grit particles (single particles or sandpaper) was found to increase the sensitivity of DAAF, allowing for the formation of ignition sites at lower firing speeds. Despite the presence of ignition sites, no propagation was observed in any DAAF sample, suggesting that although localized heating generates ignition sites during the crushing process it is not enough to sustain a propagation event. Contrary to DAAF, HMX was shown to propagate to a deflagration event even at the lowest firing speed. In the DAAF crush gun tests, the lack of observed propagation suggests that even though drop hammer testing generates enough sound to cross the threshold considered for a "go", this reaction may not involve a true propagation event in the same sense as more sensitive materials such as HMX. We suggest exploring further diagnostics (such as visible, thermal, gas production, or mechanical sensing) when evaluating an explosive that exhibits a large amount of scatter in drop-weight impact testing sound data or when more information is needed on ignition and propagation behavior.

AUTHOR INFORMATION

Corresponding Authors

Virginia W. Manner − *High Explosives Science & Technology, Los Alamos National Laboratory, Los Alamos, New Mexico 87545, United States;* orcid.org/0000-0002-1916-4887; Email: vwmanner@lanl.gov

Elizabeth G. Francois − *High Explosives Science & Technology, Los Alamos National Laboratory, Los Alamos, New Mexico 87545, United States*; Email: elizabethf@lanl.gov

https://doi.org/10.1021/acsmaterialsau.1c00013
ACS Mater. Au 2021, 1, 116−129

Authors

Nicholas Lease − *High Explosives Science & Technology, Los Alamos National Laboratory, Los Alamos, New Mexico 87545, United States;* orcid.org/0000-0001-5932-8885

Matthew D. Holmes − *Explosive Applications and Special Projects, Los Alamos National Laboratory, Los Alamos, New Mexico 87545, United States*

Michael A. Englert-Erickson − *Explosive Applications and Special Projects, Los Alamos National Laboratory, Los Alamos, New Mexico 87545, United States*

Lisa M. Kay − *High Explosives Science & Technology, Los Alamos National Laboratory, Los Alamos, New Mexico 87545, United States*

Complete contact information is available at: https://pubs.acs.org/10.1021/acsmaterialsau.1c00013

Notes

The authors declare no competing financial interest.

■ ACKNOWLEDGMENTS

The authors would like to acknowledge Danielle Montanari for help with the crush gun setup and Spencer Anthony, Ed Roemer, Clay Tiemann, Ernie Hartline, Geoff Brown, and DET-1 for particle size analysis, pellet pressing, SEM imaging, and helpful discussions. This work was supported by the US Department of Energy through the Los Alamos National Laboratory. Los Alamos National Laboratory is operated by Triad National Security, LLC, for the National Nuclear Security Administration of the U.S. Department of Energy (contract no. 89233218CNA000001). The authors would like to thank the Detonation Science & Technology group and the LANL Campaign 2 program for funding. Approved for public release (LA-UR-21-23744).

■ REFERENCES

(1) *Recommendations on the Transport of Dangerous Goods: Manual of Tests and Criteria*, 5th ed.; United Nations: New York, NY, 2009.

(2) Keshavarz, M. H.; Klapötke, T. M. *The Properties of Energetic Materials: Sensitivity, Physical and Thermodynamic Properties*, 1st ed.; De Gruyter: Berlin, Germanyy, 2018; pp 91−94.

(3) Aina, A. A.; Misquitta, A. J.; Phipps, M. J. S.; Price, S. L. "Charge Distribution of Nitro Groups within Organic Explosive Crystals: Effects on Sensitivity and Modeling". *ACS Omega* **2019**, *4* (5), 8614−8625.

(4) Yan, Q.-L.; Zeman, S. "Theoretical evaluation of sensitivity and thermal stability for high explosives based on quantum chemistry methods: A brief review. *Int. J. Quantum Chem.* **2013**, *113*, 1049−1061.

(5) Mathieu, D. "Toward a Physical Based Quantitative Modeling of Impact Sensitivities". *J. Phys. Chem. A* **2013**, *117* (10), 2253−2259.

(6) Cawkwell, M. J.; Manner, V. W. Ranking the drop-weight impact sensitivity of common explosives using Arrhenius chemical rates computed from quantum molecular dynamics simulations. *J. Phys. Chem. A* **2020**, *124*, 74−81.

(7) Gruhne, M. S.; Lommel, M.; Wurzenberger, M. H. H.; Szimhardt, N.; Klapotke, T. M.; Stierstorfer, J. OZM Ball Drop Impact Tester (BIT-132) vs. BAM Standard Method − a Comparative Investigation. *Propellants, Explos., Pyrotech.* **2020**, *45*, 147−153.

(8) Explosives Safety; DOE-STD-1212-2012; U.S. Department of Energy: Washington, D.C., 2012.

(9) Suceska, M. *Test Methods for Explosives*; Springer: Heidelberg, Germany, 1995.

(10) *Recommendations on the Transport of Dangerous Goods: Manual of Tests and Criteria*, 5 ed.; United Nations: New York, NY, 2009; pp 75−89

(11) Koenen, H.; Ide, K. H.; Swart, K.-H. Sicherheitstechnische Kenndaten explosionsf.higer Stoffe. 1: Prifverfahren der Bundesanstalt fìr Materialprifung (BAM) Berlin-Dahlem. *Explosivstoffe* **1961**, *9*, 30−42.

(12) Trimborn, F. Mechanische Messungen am großen Fallhammer der Bundesanstalt fìr Materialprìfung (BAM). *Explosivstoffe* **1970**, *18*, 49−56.

(13) Petersen, R. *Susceptibility Index of Explosives to Accidental Ignition*, NWSY-TR-81-6; Naval Weapons Station: Yorktown, VA, 1981.

(14) Simpson, L. R.; Foltz, M. F. *LLNL Small-Scale Drop-hammer Impact Sensitivity Test*, UCRL-ID-119665; Lawrence Livermore National Laboratory: Livermore, CA, 1995.

(15) Robertson, R. Some War Developments of Explosives. *Nature* **1921**, *107*, 524−527.

(16) Mortlock, H. N.; Wilby, J. The Rotter Apparatus for the Determination of Impact Sensitiveness. *Explosivstoffe* **1966**, *14*, 49−55.

(17) Klapötke, T. M.; Rienäcker, C. M. Drophammer Test Investigations on Some Inorganic and Organic Azides. *Propellants, Explos., Pyrotech.* **2001**, *26*, 43−47.

(18) Lease, N.; Kay, L. M.; Brown, G. W.; Chavez, D. E.; Leonard, P. W.; Robbins, D.; Manner, V. W. "Modifying Nitrate Ester Sensitivity Properties Using Explosive Isomers". *Cryst. Growth Des.* **2019**, *19* (11), 6708−6714.

(19) Brown, G. W.; Sandstrom, M. M.; Preston, D. N.; Pollard, C. J.; Warner, K. F.; Sorensen, D. N.; Remmers, D. L.; Phillips, J. J.; Shelley, T. J.; Reyes, J. A.; Hsu, P. C.; Reynolds, J. G. Statistical Analysis of an Inter-Laboratory Comparison of Small-Scale Safety and Thermal Testing of RDX. *Propellants, Explos., Pyrotech.* **2015**, *40*, 221−232.

(20) Doherty, R. M.; Watt, D. S. Relationship Between RDX Properties and Sensitivity. *Propellants, Explos., Pyrotech.* **2008**, *33*, 4−13.

(21) Lease, N.; Kay, L. M.; Brown, G. W.; Chavez, D. E.; Robbins, D.; Byrd, E. F. C.; Imler, G. H.; Parrish, D. A.; Manner, V. W. "Synthesis of Erythritol Tetranitrate Derivatives: Functional Group Tuning of Explosive Sensitivity". *J. Org. Chem.* **2020**, *85*, 4619−4626.

(22) Marrs, F. W.; Manner, V. W.; Burch, A. C.; Yeager, J. D.; Brown, G. W.; Kay, L. M.; Buckley, R. T.; Anderson-Cook, C.; Cawkwell, M. J. Variability in Sensitivity Testing of Pentaerythritol Tetranitrate. *Ind. Eng. Chem. Res.* **2021**, *60* (13), 5024−5033.

(23) Avrami, L.; Kirshenbaum, M. S. *Us (Arradcom) Test Results for Nato Round-Robin Test on High Explosives*, ARLCD-TR- 81010; Large Caliber Weapon Systems Laboratory: Dover, NJ, 1981.

(24) Bowes, R., Hazard Analysis of Pyrotechnic Compositions. In *2nd International Symposium on Fireworks*, Vol. *1*; Contestabile, E., Ed.; Ministry of Supply and Services: Vancouver, Canada, 1994; pp 19−31.

(25) Coffey, C. S.; DeVost, V. F. "Impact Testing of Explosives and Propellants. *Propellants, Explos., Pyrotech.* **1995**, *20*, 105−115.

(26) Smith, L. C., Problem of Evaluating the Safety of an Explosive. In *Procroceedings of the Conference on the Standardization of Safety and Performance Tests for Energetic Materials*, Vol.*1*; Avrami, L., Matsugama, H. J., Walker, R. F., Eds.; US Army Armament Research and Development Command: Dover, NJ), 1977;pp 397−414.

(27) Alouaamari, M.; Lefebvre, M. H.; Perneel, C.; Herrmann, M. Statistical Assessment Methods for the Sensitivity of Energetic Materials. *Propellants, Explos., Pyrotech.* **2008**, *33*, 60−65.

(28) Rae, P. J.; Dickson, P. M. Some Observations About the Drop-weight Explosive Sensitivity Test. *J. dynamic behavior mater* **2020**, DOI: 10.1007/s40870-020-00276-2.

(29) Reynolds, J. G.; Hsu, P. C.; Hust, G. A.; Strout, S. A.; Springer, H. K. Hot Spot Formation in Mock Materials in Impact Sensitivity Testing by Drop Hammer. *Propellants, Explos., Pyrotech.* **2017**, *42*, 1303−1308.

(30) Bowden, F. P.; Mulcahy, M. F. R.; Vines, R. G.; Yoffe, A. The detonation of liquid explosives by gentle impact. The effect of minute gas spaces. *Proc. R. Soc. A* **1947**, *188*, 291−311.
(31) Bowden, F. P.; Gurton, O. A. Initiation of solid explosives by impact and friction: the influence of grit. *Proc. R. Soc. A* **1949**, *198*, 337−349.
(32) Yoffe, A. Influence of entrapped gas on initiation of explosion in liquids and solids. *Proc. R. Soc. A* **1949**, *198*, 373−388.
(33) Blackwood, J. D.; Bowden, F. P. The initiation, burning and thermal decomposition of gunpowder. *Proc. R. Soc. A* **1952**, *213*, 285−306.
(34) Field, J. E.; Bourne, N. K.; Palmer, S. J. P.; Walley, S. M. Hotspot ignition mechanisms for explosives and propellants. *Philos. Trans. R. Soc. London A* **1992**, *339*, 269−283.
(35) Kennedy, J. E. Impact and Shear Ignition By Nonshock Mechanisms. In *Non-Shock Initiation of Explosives*, Vol. *5*; Asay, B., Ed.; Springer-Verlag, 2010); pp 555−581.
(36) Lai, W.-P.; Lian, P.; Wang, B.-Z.; Ge, Z.-X. New Correlations for Predicting Impact Sensitivities of Nitro Energetic Compounds. *J. Energ. Mater.* **2010**, *28*, 45−76.
(37) Sikder, A. K.; Sikder, N. A Review of Advanced High Performance, Insensitive and Thermally Stable Energetic Materials Emerging for Military and Space Applications″. *J. Hazard. Mater.* **2004**, *112*, 1−15.
(38) Lease, N.; Kay, L.; Chavez, D. E.; Robbins, D.; Manner, V. W. ″Increased Handling Sensitivity of Molten Erythritol Tetranitrate (ETN)″. *J. Hazard. Mater.* **2019**, *367*, 546−549.
(39) Liu, J.; Jiang, W.; Yang, Q.; Song, J.; Hao, G.; Li, F.-S. Study of Nano-Nitramine Explosives: Preparation, Sensitivity and Application″. *Defense Technology* **2014**, *10*, 184−189.
(40) Song, X.; Li, F. ″Dependence of Particle Size and Size Distribution on Mechanical Sensitivity and Thermal Stability of Hexahydro-1,3,5-trinitro-1,3,5-triazine″. *Def. Sci. J.* **2009**, *59*, 37−42. (c) Matyas, R.; Pachman, J. *Primary Explosives*; Springer, New York, NY, 2013; p 27.
(41) Reynolds, J. G.; Hsu, P. C.; Hust, G. A.; Strout, S. A.; Springer, H. K. Hot Spot Formation in Mock Materials in Impact Sensitivity Testing by Drop Hammer. *Propellants, Explos., Pyrotech.* **2017**, *42*, 1303−1308.
(42) Reynolds, J. G.; Hsu, P. C.; Hust, G. A.; Strout, S. A.; Hoffman, D. M.; Springer, H. K. Effect of Sandpaper and Grain Size on Non-Shock Initiated Reactions in HMX. *Propellants, Explos., Pyrotech.* **2017**, *42*, 1191−1202.
(43) Heatwole, E.; Parker, G.; Holmes, M.; Dickson, P. Grit mediated frictional ignition of a polymer-bonded explosive during oblique impacts: Probability calculations for safety engineering. *Reliability Engineering and System Safety* **2015**, *134*, 10−18.
(44) Manner, V.W.; Tiemann, C. G.; Yeager, J. D.; Kay, L. M.; Lease, N.; Cawkwell, M. J.; Brown, G.W.; Anthony, S. P.; Montanari, D., Examining explosives handling sensitivity of trinitrotoluene (TNT) with different particle sizes. In *Shock Compression of Condensed Matter-2019*, Vol *2272*; Armstrong, M. R., Germann, T. C., Lane, J. M. D., Eds.; American Institute of Physics: Melville, NY, 2020; 50015.
(45) Coburn, M. Picrylamino-Substituted Hetercycles. II. Furazan (1,2). *J. Heterocycl. Chem.* **1968**, *5*, 83.
(46) Solodyuk, G. D.; Boldyrev, M. D.; Gidaspov, B. V.; Nikolaev, V. D. Oxidation of 3,4-Diaminofurazan by Some Peroxide Reagents. *Zh. Org. Khim.* **1980**, *17*, 861.
(47) Francois, E. G.; Chavez, D. E.; Sandstrom, M. M. The Development of a New Synthesis Process for 3,3′-Diamino-4,4′-azoxyfurazan (DAAF). *Propellants, Explos., Pyrotech.* **2010**, *35*, 529−534.
(48) Depiero, S.; Koerner, J.; Maienschein, J.; Weese, R. Small-scale safety and thermal characterization of 3,3'-diamino-4,4'-azoxyfurazan, UCRL-TR-231649; Lawrence Livermore National Laboratories: Livermore, CA, 2007.
(49) Chellappa, R. S.; Dattelbaum, D. M.; Coe, J. D.; Velisavljevic, N.; Stevens, L. L.; Liu, Z. Intermolecular Stabilization of 3,3′-Diamino- 4,4′-azoxyfurazan (DAAF) Compressed to 20 GPa. *J. Phys. Chem. A* **2014**, *118*, 5969−5982.
(50) Wang, L. X.; Tuo, X. L.; Zou, H. T.; Yi, C. H.; Wang, X. G. Ab initio study of the molecular structure and thermal cis-trans isomerization of 3,3′-diamino-4,4′-azofurazan and 3,3′-diamino-4,4′-azoxyfurazan. *J. Theor. Comput. Chem.* **2009**, *08*, 507−17.
(51) Koch, E.-C. Insensitive High Explosives II: 3,3′-Diamino-4,4′-azoxyfurazan (DAAF). *Propellants, Explos., Pyrotech.* **2016**, *41*, 526−538.
(52) Chavez, D.; Hill, L.; Hiskey, M.; Kinkead, S. Preparation and Properties of Azo- and Azoxy-Furazans. *J. Energ. Mater.* **2000**, *18*, 219.
(53) Hiskey, M. A.; Chavez, D. E.; Bishop, R. L.; Kramer, J. F.; Kinkead, S. A. Use of 3,3′-Diamino-4,4′-azoxyfurazan and 3,3′-Diamino-4,4′-azofurazan as Insensitive High Explosive Materials. US 6358339 B1, 2002.
(54) Bowden, P. R.; Tappan, B. C.; Schmitt, M. M.; Lebrun, R. W.; Shorty, M.; Leonard, P. W.; Lichthardt, J. P.; Francois, E. G.; Hill, L. G. Synthesis, formulation and performance evaluation of reduced sensitivity explosives. *AIP Conf. Proc.* **2017**, 100005.
(55) Los Alamos National Lab batch 500-45-36.
(56) Personal communication with Rajen Patel, Picatinny Arsenal. Los Alamos National Lab batch DAAFox RDD-16F-055-051.
(57) International Organization of Standardization. *ISO Standard Particle Size Analysis—Laser Diffraction Methods: Part 1. General Principle*; ISO 13320-1:1999; Geneva, Switzerland, 1999
(58) Xu, R.; Di Guida, O. A. *Powder Technol.* **2003**, *132*, 145−153.
(59) Neyer, B. T. A D-Optimality-Based Sensitivity Test. *Technometrics* **1994**, *36*, 61.
(60) Lease, N.; Kay, L.; Chavez, D. E.; Robbins, D.; Manner, V. W. Increased Handling Sensitivity of Molten Erythritol Tetranitrate. *J. Hazard. Mater.* **2019**, *367*, 546−549.
(61) Walley, S. M.; Field, J. E.; Biers, R. A.; Proud, W. G.; Williamson, D. M.; Jardine, A. P. The Use of Glass Anvils in Drop-Weight Studies of Energetic Materials. *Propellants, Explos., Pyrotech.* **2015**, *40*, 351−365.
(62) Bowden, F. P.; Gurton, O. A. Birth and Growth of Explosion in Liquids and Solids Initiated by Impact and Friction. *Proc. R. Soc. London A* **1949**, *198*, 350−372.
(63) Field, J. E.; Swallowe, G. M.; Heavens, S. N. Ignition Mechanisms of Explosives During Mechanical Deformation. *Proc. R. Soc. London A* **1982**, *382*, 231−244.
(64) Heavens, S. N. *The Initiation of Explosion by Impact*, PhD Thesis, University of Cambridge, Cambridge, England, 1973.
(65) Swallowe, G. M.; Field, J. E. The Ignition of a Thin Layer of Explosive by Impact: The Effect of Polymer Particles. *Proc. R. Soc. London A* **1982**, *379*, 389−408.
(66) Swallowe, G. M.; Field, J. E. Effect of Polymers on the Dropweight Sensitiveness of Explosives. In *7th Symposium (International) on Detonation*; Short, J. M., Ed.; Naval Surface Weapons Center: Dahlgren, VA, 1981; pp 24−35.
(67) Perry, W. L.; Gunderson, J. A.; Balkey, M. M.; Dickson, P. M. Impact-Induced Friction Ignition of an Explosive: Infrared Observations and Modeling. *J. Appl. Phys.* **2010**, *108* (8), 084902−1−084902−8.
(68) Winter, R. E.; Field, J. E. The role of localized plastic flow in the impact initiation of explosives. *Proc. R. Soc. London, Ser. A* **1975**, *343*, 399−413.
(69) Field, J. E.; Palmer, S. J. P.; Pope, P. H.; Sundararajan, R.; Swallowe, G. M. Mechanical properties of PBX's and their behavior during drop-weight impact. *Proc. 8th. Symp. (Int.) on Detonation* **1985**, 635−644.
(70) Walley, S. M.; Field, J. E.; Biers, R. A.; Proud, W. G.; Williamson, D. M.; Jardine, A. P. The use of glass anvils in drop weight studies of energetic materials. *Propellants, Explos., Pyrotech.* **2015**, *40*, 351−365.
(71) The contact pressure reduces the discrepancy in the refraction indices, increasing reflectance off the sample material and reducing the reflectance off the internal sapphire surface.

https://doi.org/10.1021/acsmaterialsau.1c00013
ACS Mater. Au 2021, 1, 116−129

(72) Sapphire is an extremely good thermal conductor, and the anvil has a large thermal mass; both serve to pull heat away from the grit−sapphire hotspot location (with one piece of grit). In contrast, the grit−grit interactions in the grit paper—as some particles become debonded but others remain adhered to the paper—is much more effective at heating; the particles are even backed by insulation in the forms of both the adhesive on the paper and the paper itself. We would anticipate that the grit−sapphire interaction would be less effective at creating hotspots.

https://doi.org/10.1021/acsmaterialsau.1c00013
ACS Mater. Au 2021, 1, 116−129